

Jet quenching with T -dependent running coupling

B.G. Zakharov^{1,2}

¹ *L.D. Landau Institute for Theoretical Physics, GSP-1, 117940,
Kosygina Str. 2, 117334 Moscow, Russia*

² *Steklov Mathematical Institute, Russian Academy of Sciences, Gubkin str. 8, 119991 Moscow, Russia*

(Dated: August 28, 2024)

We perform an analysis of jet quenching in heavy ion collisions at RHIC and LHC energies with the temperature dependent running QCD coupling. Our results show that the T -dependent QCD coupling largely eliminates the difference between the optimal values of α_s for the RHIC and LHC energies. It may be viewed as direct evidence of the increase of the thermal suppression of α_s with rising temperature.

PACS numbers:

1. Introduction. It is accepted that the strong suppression of the high- p_T particle spectra in AA collisions (usually called the jet quenching) observed at RHIC and LHC, is due to parton energy loss (radiative and collisional) in the quark-gluon plasma (QGP). The jet quenching is one of the major signals of the QGP formation in relativistic AA collisions. The main contribution to the parton energy loss comes from the radiative mechanism due to induced gluon emission [1–5]. The effect of the collisional energy loss turns out to be relatively weak [6, 7].

The available pQCD approaches to the radiative energy loss [1–5] are limited to the one gluon emission. The effect of multiple gluon radiation is usually accounted for in the approximation of independent gluon emission [8]. Altogether, the pQCD calculations within this approximation give a rather good agreement with the jet quenching data from RHIC and LHC (see e.g. [9] and references therein). However, it was found that, in the formulation with a unique temperature independent QCD coupling, the simultaneous description of the RHIC and LHC data requires to use somewhat smaller α_s at the LHC energies [9–12] (in [13, 14] a similar difference between jet quenching at RHIC and LHC energies, has been found in terms of the transport coefficient \hat{q}). In [9–12] this fact has been demonstrated within the light-cone path integral (LCPI) approach to induced gluon emission [2], using the method developed in [15, 16], for running α_s which is frozen at low momenta at some value α_s^{fr} . There it was found that the RHIC data support a significantly larger value of α_s^{fr} than the LHC data. One of the reasons for this difference may be somewhat stronger thermal suppression of the effective QCD coupling in a hotter QGP at the LHC energies. To draw a firm conclusion on this possibility it is highly desirable to perform calculations with a temperature dependent α_s . And of course, it is clear that, even without respect to the problem with a joint description of the RHIC and LHC jet quenching data, an observation of the temperature dependence of α_s from the jet quenching data would be of great importance on its own. The case of the T -dependent coupling has not been discussed so far in the literature on jet quenching. The purpose of this work is to perform such an analysis. We adapt the LCPI formalism to the case of the T -dependent running α_s , and perform a joint analysis of the jet quenching data from RHIC on 0.2 TeV Au+Au collisions and from the LHC on 5.02 TeV Pb+Pb collisions.

2. Theoretical framework. We will consider the central rapidity region around $y = 0$. Our method for calculating the nuclear modification factor R_{AA} is similar to the one used in our previous jet quenching analyses [9, 12, 16]. Therefore, we only outline its main points. We write the nuclear modification factor R_{AA} for given impact parameter b of AA collision, the hadron transverse momentum \mathbf{p}_T and rapidity y as

$$R_{AA}(b, \mathbf{p}_T, y) = \frac{dN(A + A \rightarrow h + X)/d\mathbf{p}_T dy}{T_{AA}(b)d\sigma(N + N \rightarrow h + X)/d\mathbf{p}_T dy}, \quad (1)$$

where $T_{AA}(b) = \int d\rho T_A(\rho)T_A(\rho - \mathbf{b})$, $T_A(\rho) = \int dz \rho_A(\sqrt{\rho^2 + z^2})$ is the nuclear thickness function (with ρ_A the nuclear density). The nominator on the right hand side of (1) is the differential yield of the process $A + A \rightarrow h + X$ (we omit for clarity the arguments b and \mathbf{p}_T). It can be written via the medium-modified hard cross section $d\sigma_m/d\mathbf{p}_T dy$ in the form

$$\frac{dN(A + A \rightarrow h + X)}{d\mathbf{p}_T dy} = \int d\rho T_A(\rho + \mathbf{b}/2)T_A(\rho - \mathbf{b}/2) \frac{d\sigma_m(N + N \rightarrow h + X)}{d\mathbf{p}_T dy}. \quad (2)$$

We write $d\sigma_m/d\mathbf{p}_T dy$ as

$$\frac{d\sigma_m(N + N \rightarrow h + X)}{d\mathbf{p}_T dy} = \sum_i \int_0^1 \frac{dz}{z^2} D_{h/i}^m(z, Q) \frac{d\sigma(N + N \rightarrow i + X)}{d\mathbf{p}_T^i dy}, \quad (3)$$

where $\mathbf{p}_T^i = \mathbf{p}_T/z$ is the transverse momentum of the initial hard parton, $d\sigma(N + N \rightarrow i + X)/d\mathbf{p}_T^i dy$ is the ordinary hard cross section, and $D_{h/i}^m(z, Q)$ is the medium-modified fragmentation function for transition of a parton i with the virtuality $Q \sim p_T^i$ to the final hadron h . The fragmentation functions $D_{h/i}^m(z, Q)$ accumulate the medium effects. They depend crucially on the QGP fireball density profile along the hard parton trajectory. We use somewhat improved method of [16] for evaluation of $D_{h/i}^m(z, Q)$ via the one gluon induced spectrum in the approximation of independent gluon emission [8]. We refer the interested reader to [9] for details. Also there, a detailed description of the technical aspects of the implementation of formulas (1)–(3) can be found.

We turn now to the method for incorporation of the temperature dependent coupling in calculating the induced gluon spectrum. Let us consider the case of $q \rightarrow gq$ process. In the LCPI formalism [2] the gluon spectrum in $x = E_g/E_q$ for $q \rightarrow gq$ process can be written as [15]

$$\frac{dP}{dx} = \int_0^L dz n(z) \frac{d\sigma_{eff}^{BH}(x, z)}{dx}, \quad (4)$$

where $n(z)$ is the medium number density, $d\sigma_{eff}^{BH}/dx$ is an effective Bethe-Heitler cross section accounting for both the Landau-Pomeranchuk-Migdal and the finite-size effects. Note that for the midrapidity region $y = 0$, the longitudinal coordinate z in (4) coincides with the proper time τ for evolution of the QGP fireball. At fixed coupling $d\sigma_{eff}^{BH}/dx$ can be written as [15]

$$\frac{d\sigma_{eff}^{BH}(x, z)}{dx} = -\frac{P_q^g(x)}{\pi M} \text{Im} \int_0^z d\xi \alpha_s \frac{\partial}{\partial \rho} \left(\frac{F(\xi, \rho)}{\sqrt{\rho}} \right) \Big|_{\rho=0}. \quad (5)$$

Here $P_q^g(x) = C_F[1 + (1-x)^2]/x$ is the usual splitting function for $q \rightarrow gq$ process, $M = Ex(1-x)$ is the reduced "Schrödinger mass", F is the solution to the radial Schrödinger equation for the azimuthal quantum number $m = 1$

$$i \frac{\partial F(\xi, \rho)}{\partial \xi} = \left[-\frac{1}{2M} \left(\frac{\partial}{\partial \rho} \right)^2 + v(\rho, x, z - \xi) + \frac{4m^2 - 1}{8M\rho^2} + \frac{1}{L_f} \right] F(\xi, \rho) \quad (6)$$

with the boundary condition $F(\xi = 0, \rho) = \sqrt{\rho} \sigma_3(\rho, x, z) \epsilon K_1(\epsilon \rho)$ (K_1 is the Bessel function), $L_f = 2M/\epsilon^2$ with $\epsilon^2 = m_q^2 x^2 + m_g^2 (1-x)^2$, $\sigma_3(\rho, x, z)$ is the cross section of interaction of the $q\bar{q}g$ system with a medium constituent located at z . The potential v in (6) reads

$$v(\rho, x, z) = -i \frac{n(z) \sigma_3(\rho, x, z)}{2}. \quad (7)$$

The σ_3 is given by [17]

$$\sigma_3(\rho, x, z) = \frac{9}{8} [\sigma_{q\bar{q}}(\rho, z) + \sigma_{q\bar{q}}((1-x)\rho, z)] - \frac{1}{8} \sigma_{q\bar{q}}(x\rho, z), \quad (8)$$

where

$$\sigma_{q\bar{q}}(\rho, z) = C_T C_F \int d\mathbf{q} \alpha_s^2 \frac{[1 - \exp(i\mathbf{q}\boldsymbol{\rho})]}{[q^2 + \mu_D^2(z)]^2} \quad (9)$$

is the local dipole cross section for the color singlet $q\bar{q}$ pair, $C_{F,T}$ are the color Casimir for the quark and thermal parton (quark or gluon), μ_D is the local Debye mass.

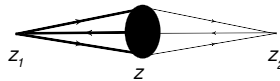


FIG. 1: Diagrammatic representation of the effective Bethe-Heitler cross section for $a \rightarrow bc$ process in terms of the dressed (left) and bare (right) Green functions describing z -evolution of the $\bar{a}bc$ system. The central blob corresponds to the potential v . Integration over z_1 (from 0 to z) and z_2 (from z to ∞) is implied.

Diagrammatically, the effective Bethe-Heitler cross section (5), for any partonic process $a \rightarrow bc$, is given by the graph shown in Fig. 1 where the left and right parts correspond to the dressed and bare Green functions describing

z -evolution of the $\bar{a}bc$ three-body system (i.e. $\bar{q}qg$ for $q \rightarrow qg$ process). The central black blob in Figs. 1 describes interaction of the three-body state with a medium constituent. For RHIC and LHC conditions the dominating contribution to the effective Bethe-Heitler cross section comes from $N = 1$ scattering. This means that the dressed Green function in Fig. 1 is close to the bare one. Therefore in this regime the average $z - z_1$ is close to $z_2 - z$. For generalization of the above formulas to the case of running T -dependent coupling one should modify α_s that appears on the right hand side of (5), which comes from product of the QCD couplings in the decay vertices at z_1 and z_2 in Fig. 1, and α_s^2 in formula for the dipole cross section (9). In the latter case it is natural simply to replace the fixed α_s by the local running coupling $\alpha_s(q, T(z))$. However, the situation is more complicated for α_s on the right hand side of (5). In terms of the variable ξ in (5) $z_1 = z - \xi$. As we said above, for the dominating $N = 1$ scattering term on the average $z - z_1 \sim z_2 - z$. We will use this approximation for the whole effective Bethe-Heitler cross section. Then, for the temperatures at the decay vertices one can take $T(z \pm \xi)$. This approximation should be reasonable due to a smooth dependence of T on the proper time ($T \propto \tau^{-1/3}$) and a smooth (logarithmic) dependence of α_s on the QGP temperature. Since we work in the coordinate space the virtualities at the decay vertices do not appear in our formulas. Qualitatively, from the uncertainty relation, one can obtain that $Q^2 \sim 1/\rho^2$, where ρ is the transverse size of the three-body state at z . Similarly to our previous analyses of jet quenching with a unique T -independent running α_s , we determine the virtuality for these vertices as $Q^2(\xi) = a/\xi$ with $a = 1.85$ [7]. This parametrization accounts for the Schrödinger diffusion relation, that gives $\rho^2 \sim \xi/M$, and the value of the parameter a has been adjusted to reproduce the $N = 1$ scattering contribution evaluated in the ordinary Feynman diagrammatic approach [18]. Thus, for calculations with the T -dependent running coupling we replace the fixed α_s on the right-hand side of (5) by $\sqrt{\alpha_s(Q(\xi), T(z - \xi))\alpha_s(Q(\xi), T(z + \xi))}$. We checked that the version with $T(z \pm \xi)$ replaced by $T(z)$ gives practically the same results, i.e. the effect of the finite separation between the decay vertices is small. This occurs because the dominating contribution to the radiative energy loss comes from gluons with the formation length which is considerably smaller than the QGP size.

First principle calculations of the $\alpha_s(Q, T)$ in the QGP are not yet available. In the lattice analysis [19], via calculation of the free energy of a static heavy quark-antiquark pair, there have been obtained an effective in-medium coupling $\alpha_s(r, T)$ in the coordinate representation. The results of [19] show that $\alpha_s(r, T)$ at $r \ll 1/T$ becomes close to the ordinary vacuum QCD coupling $\alpha_s(Q)$ with $Q \sim 1/r$. In the infrared region $\alpha_s(r, T)$ reaches maximum at $r \sim 1/\kappa T$ with $\kappa \sim 4$ and then with increasing r it falls to zero. With identification $r \sim 1/Q$, this pattern is qualitatively similar to that obtained for $\alpha_s(Q, T)$ in the momentum representation within the functional renormalization group calculations [20]. Motivated by the results of [19, 20], we use parametrization of $\alpha_s(Q, T)$ in the form

$$\alpha_s(Q, T) = \begin{cases} \frac{4\pi}{9 \log(Q^2/\Lambda_{QCD}^2)} & \text{if } Q > Q_{fr}(T), \\ \alpha_s^{fr}(T) & \text{if } Q_{fr}(T) \geq Q \geq cQ_{fr}(T), \\ \alpha_s^{fr}(T) \times (Q/cQ_{fr}(T)) & \text{if } Q < cQ_{fr}(T), \end{cases} \quad (10)$$

where $Q_{fr} = \Lambda_{QCD} \exp\{2\pi/9\alpha_s^{fr}\}$ (in the present analysis we take $\Lambda_{QCD} = 200$ MeV), and $c < 1$. The parameter c defines the width of the plateau where α_s equals its maximum value α_s^{fr} . For our basic version we take $c = 0.8$. We have also performed calculations for $c = 0$. The case $c = 0$ is similar to the model with a frozen QCD coupling in the infrared region at $T = 0$ [21, 22]. In [22] it was called the F -model. For $c \sim 1$ the parametrization (10) is qualitatively similar to the G -model of the vacuum α_s of [22]. We take $Q_{fr} = \kappa T$, and perform fit of the free parameter κ using the data on the nuclear modification factor R_{AA} . From the lattice results of [19] one can expect that $\kappa \sim 4$. But since the relation $r \sim 1/Q$ is of qualitative nature, our parameter κ may differ from that in the lattice calculations in the coordinate space. Also, one should bear in mind that in the infrared region the effective coupling becomes process dependent [19]. We also present the results for a unique α_s in the whole QGP with the T -independent free parameter α_s^{fr} .

3. Numerical results. We perform calculations for the QGP fireball with purely longitudinal Bjorken's 1+1D expansion [23], which gives proper time dependence of the entropy density $s(\tau)/s(\tau_0) = \tau_0/\tau$, where τ_0 is the QGP thermalization time. We take $\tau_0 = 0.5$ fm. As in [9] we take a linear τ -dependence $s(\tau) = s(\tau_0)\tau/\tau_0$ for $\tau < \tau_0$. We neglect variation of the initial QGP density with the transverse coordinates across the overlapping area of two colliding nuclei. The average initial temperature has been evaluated in the Glauber wounded nucleon model [24] (with parameters from [25, 26]). For central collisions this gives $T_0 \sim 320(420)$ MeV for 0.2 TeV Au+Au(5.02 TeV Pb+Pb) collisions. We refer the reader to [9] for more details on the model and parameters of the QGP fireball. For the T -dependence of α_s and the Debye mass we use the temperature extracted from the entropy $s(\tau)$ using the lattice entropy density obtained in [27]. For a given entropy, this temperature is somewhat larger than the ideal gas temperature. As in [9], we use the Debye mass obtained in the lattice analysis [28], and take $m_q = 300$ and $m_g = 400$ MeV for the light quark and gluon quasiparticle masses in the QGP [29].

We have performed the χ^2 fit of the free parameters κ/α_s^{fr} using the the RHIC and LHC data on R_{AA} for centralities

	$\alpha_s(Q, T)$		$\alpha_s(Q)$	
	κ	$\chi^2/d.p.$	α_s^{fr}	$\chi^2/d.p.$
PHENIX Au+Au 0.2 TeV	2.65	0.167(0.71, 0.81)	0.698	0.157(4.4, 4.75)
ALICE Pb+Pb 5.02 TeV	3.19	0.46(0.68)	0.464(0.464)	0.56(0.88)
ATLAS Pb+Pb 5.02 TeV	3.48(3.46)	0.37(0.22)	0.439(0.439)	0.33(0.2)
CMS Pb+Pb 5.02 TeV	3.99(3.81)	0.58(0.25)	0.403(0.412)	0.46(0.21)
All LHC Pb+Pb 5.02 TeV	3.33(3.28)	1.04(0.96)	0.451(0.455)	0.93(0.96)

TABLE I: Optimal values of κ and α_s^{fr} (for $c = 0.8$ in formula (10)) and corresponding $\chi^2/d.p.$ for different data sets. For LHC the results are presented for fits for the data points with $9 < p_T < 120$ and $9 < p_T < 22$ GeV (the numbers in brackets). For RHIC the fits are performed for the data points with $p_T > 9$ GeV. The numbers in brackets for $\chi^2/d.p.$ for RHIC give $\chi^2/d.p.$ obtained with the LHC optimal parameters κ/α_s^{fr} obtained for the LHC fits for $9 < p_T < 22$ GeV and $9 < p_T < 120$ GeV.

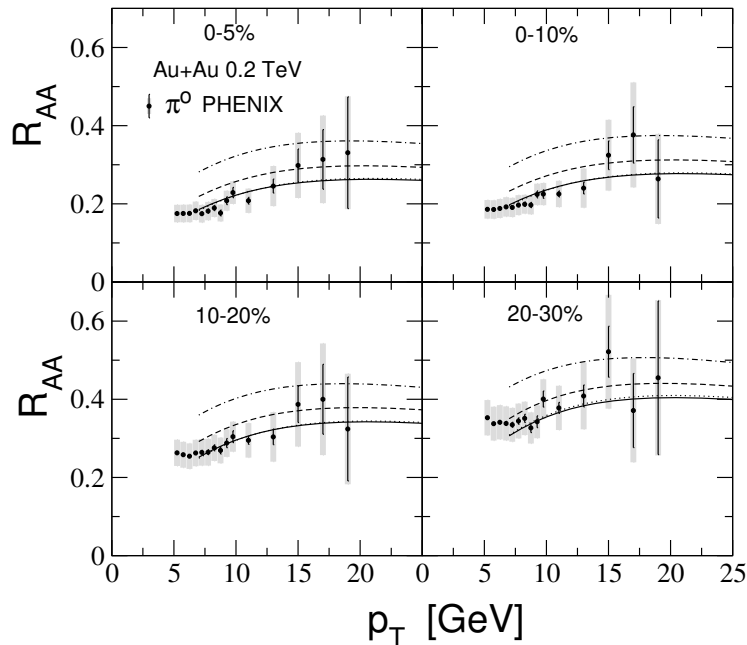


FIG. 2: R_{AA} of π^0 for 0.2 TeV Au+Au collisions for different centrality bins from our calculations for T -dependent α_s (solid and dashed) and T -independent α_s (dotted and dash-dotted) compared to data from PHENIX [30]. The solid and dotted curves are for $\kappa = 2.65$ and $\alpha_s^{fr} = 0.698$ obtained by fitting the PHENIX R_{AA} data set for $p_T > 9$ GeV. The dashed and dash-dotted lines are for $\kappa = 3.28$ and $\alpha_s^{fr} = 0.455$ obtained by fitting the LHC R_{AA} data sets for $9 < p_T < 22$ GeV.

smaller than 30%. We use the data for 0.2 TeV Au+Au collisions at RHIC from PHENIX [30] for π^0 -meson and for 5.02 TeV collisions Pb+Pb at the LHC from ALICE [31], ATLAS [32], and CMS [33] for charged hadrons. We take $p_{T,min} = 9$ GeV¹. For the PHENIX data [30] we include all data points with $p_T > p_{T,min}$. For the LHC data we perform fitting for $p_{T,max} = 120$ and 22 GeV. The latter value seems to be preferable for studying the variation of α_s from RHIC to LHC, since for the PHENIX data $p_T < 20$ GeV. But we have found that the LHC fits for $p_{T,max} = 120$ and 22 GeV give very similar results. We calculate χ^2 as

$$\chi^2 = \sum_i^N \frac{(f_i^{exp} - f_i^{th})^2}{\sigma_i^2}, \quad (11)$$

¹ The χ^2 fits with $p_{T,min} \sim 7 - 10$ GeV give very similar results. However, the inclusion of the data points with $p_T \lesssim 7 - 8$ GeV does not make sense, since at such p_T the non-fragmentation recombination mechanism [34, 35] may become important. It is quite likely that just this mechanism causes the growth of R_{AA} at $p_T \lesssim 6 - 7$ GeV for the LHC energies.

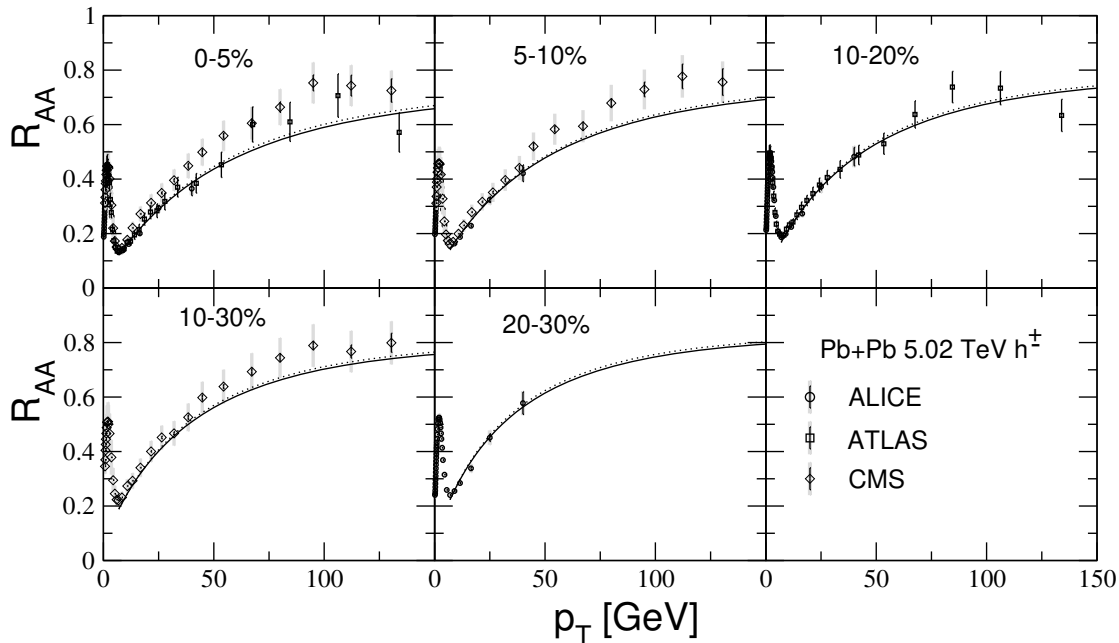


FIG. 3: R_{AA} of charged hadrons for 5.02 TeV Pb+Pb collisions for different centrality bins. Solid: calculations for T -dependent α_s with $\kappa \approx 3.33$. Dotted: calculations for T -independent α_s with $\alpha_s^{fr} \approx 0.451$. κ and α_s^{fr} are obtained by fitting R_{AA} in the range $9 < p_T < 120$ GeV. Data points are from ALICE [31], ATLAS [32], and CMS [33].

where N is the number of the data points, the squared errors include the systematic and statistic errors $\sigma_i^2 = \sigma_{i,stat}^2 + \sigma_{i,sys}^2$. In calculating χ^2 as functions of free parameters κ and α_s^{fr} we have used the theoretical R_{AA} obtained with the help of a cubic spline interpolation from the grids calculated with steps (in κ and α_s^{fr}) $\Delta\kappa/\kappa, \Delta\alpha_s^{fr}/\alpha_s^{fr} \sim 0.05$. The optimal values of κ and α_s^{fr} with corresponding values of $\chi^2/d.p.$ (χ^2 per data point) are summarized in Table I. In Table I we show the results for RHIC and LHC separately. We also performed fitting for the combined RHIC plus LHC data set (not shown). In this case the results are very close to that for the LHC data set alone. This occurs because the number of the data points for the LHC data set is much bigger than for the RHIC data set. From Table I one can see that the LHC data give somewhat bigger value of the optimal parameter κ . However, the difference is not very big. To illustrate better the difference between RHIC and LHC, in Table I for the PHENIX data set besides $\chi^2/d.p.$ for κ and α_s^{fr} fitted to the PHENIX data we also give $\chi^2/d.p.$ for the optimal κ and α_s^{fr} obtained for the LHC data set. One can see that for the T -dependent α_s the LHC value of κ gives rather good fit quality $\chi^2/d.p. \approx 0.7 - 0.8$, while for the T -independent α_s for the LHC optimal parameter α_s^{fr} we have $\chi^2/d.p. \approx 4.4 - 4.8$, that says about a rather strong disagreement with the PHENIX data.

In Figs. 2–3 we compare our results for R_{AA} with the RHIC data from PHENIX for π^0 -meson in 0.2 TeV Au+Au collisions [30] and the LHC data [31–33] for h^\pm in 5.02 TeV Pb+Pb collisions. One can see that for the optimal parameters (separately for RHIC and LHC) agreement with the data is quite good for both the versions. However, the situation with a joint description of the RHIC and LHC data is very different for the T -dependent and T -independent couplings. To visualize better this difference in Fig. 2, in addition to predictions for R_{AA} in Au+Au collisions obtained with the optimal parameters fitted to the PHENIX data, we also plot the results for the optimal parameters fitted to the LHC data. As one can see, for the version with T -dependent coupling the LHC value of κ leads to not bad agreement with the PHENIX data. While for the version with T -independent coupling the curves for the LHC value of α_s^{fr} overshoot the data considerably at $p_T \lesssim 15$ GeV. For the T -dependent version some overshooting at $p_T \lesssim 15$ GeV also exists, but it is rather small. We conclude from comparison with experimental data shown in Figs. 2–3 and results of our fits given in Table I, that the T -dependence of the QCD coupling may strongly reduce the difference between the optimal α_s for RHIC and LHC². We have checked that, in principle, for the T -dependent

² Note that for the LHC data on 2.76 TeV Pb+Pb collisions [36–38] the situation is the same. Our calculations show that the optimal parameters (and quality of the fits) in this case are very close to that for 5.02 TeV Pb+Pb collisions.

coupling by a relatively small increase of $\alpha_s(Q, T)$ at $Q \sim (1-3)\Lambda_{QCD}$, as compared to the one-loop formula used in (10), for κ fitted to the LHC data one can significantly improve agreement with the RHIC data in the low p_T region. Such an increase of the $\alpha_s(Q, T)$ is not unrealistic, e.g., it may mimic an enhancement of the induced gluon emission at $T \sim T_c$ [39, 40] in the presence color-magnetic monopoles [41].

We have also calculated the azimuthal asymmetry v_2 . Although we have fitted the optimal parameters to the data on R_{AA} , for both the T -dependent and T -independent versions we have obtained a quite reasonable agreement with the v_2 data as well. For the T -dependent version, we obtained a bit bigger v_2 . This occurs due to some enhancement of the contribution to the energy loss from the later, low temperature, stage of the QGP evolution, which has a bigger initial fireball azimuthal asymmetry.

The above results have been obtained for parametrization (10) with $c = 0.8$. The results from calculation for $c = 0$ in (10), i.e. for flat α_s at $Q < Q_{fr}$, turn out to be very similar to that for $c = 0.8$. We obtained rather good agreement with the RHIC and LHC data for the versions with T -dependent and T -independent coupling. However, similarly to the case $c = 0.8$, the latter version leads to a considerable disagreement between free parameters for RHIC and LHC. While the former version largely eliminates this disagreement.

4. Summary. We have studied the influence of the temperature dependence of running coupling on the variation of jet quenching from the RHIC to LHC energies within the LCPI [2] approach to the induced gluon emission. The calculations are performed using the method suggested in [15, 16]. For our basic version we use parametrization of running coupling $\alpha_s(Q, T)$ which has a short plateau α_s^{fr} around $Q_{fr} \sim \kappa T$, and then falls $\propto Q$ at small Q . This ansatz is motivated by the lattice calculation of the effective QCD coupling in the QGP [19] and the results obtained within the functional renormalization group [20]. We have determined the optimal values of the parameter κ fitting the data on the nuclear modification factor R_{AA} in 0.2 TeV Au+Au collisions at RHIC and in 5.02 TeV Pb+Pb collisions at the LHC. We have found that the RHIC data require somewhat smaller value of the parameter κ than the LHC data. But nevertheless the theoretical R_{AA} for 0.2 Au+Au collisions calculated with the optimal κ adjusted to fit the LHC data, is in reasonable agreement with the RHIC data ($\chi^2/d.p. \approx 0.7-0.8$). This differs drastically from the results for the T -independent α_s^{fr} , which leads to rather strong disagreement with the RHIC data ($\chi^2/d.p. \approx 4.4-4.8$) for the optimal value α_s^{fr} fitted to the LHC data. Thus, our analysis shows that the T -dependent α_s may largely eliminate the problem of different optimal QCD coupling for the RHIC and LHC energies. For parametrization with flat α_s at $Q < Q_{fr}$ with $Q_{fr} = \kappa T$ we obtained very similar results. Our results may be viewed as the first direct evidence of the increase of the thermal suppression of α_s with rising QGP temperature.

Acknowledgments

This work was performed under the Russian Science Foundation grant 20-12-00200 at Steklov Mathematical Institute.

-
- [1] R. Baier, Y.L. Dokshitzer, A.H. Mueller, S. Peigné, and D. Schiff, Nucl. Phys. B**483**, 291 (1997) [arXiv:hep-ph/9607355].
 - [2] B.G. Zakharov, JETP Lett. **63**, 952 (1996) [arXiv:hep-ph/9607440].
 - [3] U.A. Wiedemann, Nucl. Phys. A**690**, 731 (2001) [arXiv:hep-ph/0008241].
 - [4] M. Gyulassy, P. Lévai, and I. Vitev, Nucl. Phys. B**594**, 371 (2001) [arXiv:hep-ph/0006010].
 - [5] P. Arnold, G.D. Moore, and L.G. Yaffe, JHEP **0206**, 030 (2002) [arXiv:hep-ph/0204343].
 - [6] R. Baier, D. Schiff, and B.G. Zakharov, Ann. Rev. Nucl. Part. Sci. **50**, 37 (2000) [arXiv:hep-ph/0002198].
 - [7] B.G. Zakharov, JETP Lett. **86**, 444 (2007) [arXiv:0708.0816].
 - [8] R. Baier, Y.L. Dokshitzer, A.H. Mueller, and D. Schiff, JHEP **0109**, 033 (2001) [arXiv:hep-ph/0106347].
 - [9] B.G. Zakharov, J. Phys. G in press [arXiv:2007.09772].
 - [10] B.G. Zakharov, J. Phys. G**38**, 124161 (2011).
 - [11] B.G. Zakharov, JETP Lett. **93**, 683 (2011) [arXiv:1105.2028].
 - [12] B.G. Zakharov, J. Phys. G**40**, 085003 (2013) [arXiv:1304.5742].
 - [13] K.M. Burke *et al.* [JET Collaboration] Phys. Rev. C**90**, 014909 (2014) [arXiv:1312.5003].
 - [14] X. Feal, C.A. Salgado, and R.A. Vazquez, [arXiv:1911.01309].
 - [15] B.G. Zakharov, JETP Lett. **80**, 617 (2004) [arXiv:hep-ph/0410321].
 - [16] B.G. Zakharov, JETP Lett. **88**, 781 (2008) [arXiv:0811.0445].
 - [17] N.N. Nikolaev and B.G. Zakharov, Z. Phys. C**64**, 631 (1994) [arXiv:hep-ph/9306230].
 - [18] B.G. Zakharov, JETP Lett. **80**, 67 (2004) [hep-ph/0406063].
 - [19] A. Bazavov *et al.*, Phys. Rev. D**98**, 054511 (2018) [arXiv:1804.10600].
 - [20] J. Braun and H. Gies, Phys. Lett. B**645**, 53 (2007) [hep-ph/0512085].
 - [21] A.C. Mattingly and P.M. Stevenson, Phys. Rev. D**49**, 437 (1994) [hep-ph/9307266].

- [22] Yu.L. Dokshitzer, V.A. Khoze, and S.I. Troyan, *Phys. Rev. D* **53**, 89 (1996) [arXiv:hep-ph/9506425].
- [23] J.D. Bjorken, *Phys. Rev. D* **27**, 140 (1983).
- [24] D. Kharzeev and M. Nardi, *Phys. Lett. B* **507**, 121 (2001) [arXiv:nucl-th/0012025].
- [25] B.G. Zakharov, *JETP* **124**, 860 (2017) [arXiv:1611.05825].
- [26] B.G. Zakharov, *Eur. Phys. J. C* **78**, 427 (2018) [arXiv:1804.05405].
- [27] S. Borsanyi, G. Endrodi, Z. Fodor, A. Jakovac, S.D. Katz, S. Krieg, C. Ratti, and K. K. Szabo, *JHEP* **1011**, 077 (2010) [arXiv:1007.2580].
- [28] O. Kaczmarek and F. Zantow, *Phys. Rev. D* **71**, 114510 (2005) [arXiv:hep-lat/0503017].
- [29] P. Lévai and U. Heinz, *Phys. Rev. C* **57**, 1879 (1998) [hep-ph/9710463].
- [30] A. Adare *et al.* [PHENIX Collaboration], *Phys. Rev. C* **87**, 034911 (2013) [arXiv:1208.2254].
- [31] S. Acharya *et al.* [ALICE Collaboration], *JHEP* **1811**, 013 (2018) [arXiv:1802.09145].
- [32] The ATLAS collaboration, ATLAS-CONF-2017-012, <http://cds.cern.ch/record/2244824?ln=en>
- [33] V. Khachatryan *et al.* [CMS Collaboration], *JHEP* **1704**, 039 (2017) [arXiv:1611.01664].
- [34] R.J. Fries, B. Muller, C. Nonaka, and S.A. Bass, *Phys. Rev. C* **68**, 044902 (2003) [nucl-th/0306027].
- [35] V. Minissale, F. Scardina, and V. Greco, *Phys. Rev. C* **92**, 054904 (2015) [arXiv:1502.06213].
- [36] B. Abelev *et al.* [ALICE Collaboration], *Phys. Lett. B* **720**, 52 (2013) [arXiv:1208.2711].
- [37] G. Aad *et al.* [ATLAS Collaboration], *JHEP* **1509**, 050 (2015) [arXiv:1504.04337].
- [38] S. Chatrchyan *et al.* [CMS Collaboration], *Eur. Phys. J. C* **72**, 1945 (2012) [arXiv:1202.2554].
- [39] J. Xu, J. Liao, and M. Gyulassy, *Chin. Phys. Lett.* **32**, 092501 (2015) [arXiv:1411.3673].
- [40] B.G. Zakharov, *JETP Lett.* **101**, 587 (2015) [arXiv:1412.6287].
- [41] J. Liao and E. Shuryak, *Phys. Rev. C* **75**, 054907 (2007) [arXiv:hep-ph/0611131].